NanoImpact 11 (2018) 146–155

Contents lists available at ScienceDirect

NanoImpact

journal homepage: www.elsevier.com/locate/nanoimpact

Research paper

Carbon nanomaterials differentially impact mineralization kinetics of phenanthrene and indigenous microbial communities in a natural soil

Haiyun Zhang[a], Fan Wu[a], Weixiao Chen[a], Xinyu Zhang[a], Pedro J.J. Alvarez[b], J. Julio Ortega-Calvo[c], Yu Yang[d], Shu Tao[a], Xilong Wang[a,*]

[a] Laboratory for Earth Surface Processes, College of Urban and Environmental Sciences, Peking University, Beijing 100871, China
[b] Department of Civil and Environmental Engineering, Rice University, Houston, TX 77005, United States
[c] Instituto de Recursos Naturales y Agrobiologia de Sevilla (IRNAS-CSIC), Spain
[d] Department of Civil and Environmental Engineering, University of Nevada, Reno, NV 89557, United States

ARTICLE INFO

Keywords:
Carbon nanomaterial
PAH
Mineralization
Indigenous microbes
Fungi

ABSTRACT

Previous reports on how carbon nanomaterials (CNMs) affect the biodegradation and mineralization of organic contaminants are mainly limited to pure culture studies, but little is known about the mineralization process by more complex and environmentally-relevant microbial communities. This study investigated the impact of fullerenes C_{60} and two multi-walled carbon nanotubes (outer diameter < 8 nm: M8; > 50 nm: M50) at 300 and 3000 mg/kg on the mineralization kinetics of ^{14}C-phenanthrene (18.5 mg/kg) by indigenous microorganisms in a natural soil for 120 days. Phenanthrene mineralization kinetics fitted well with the logistic growth equation regardless of the CNMs present (R^2 = 0.965–0.985). The maximum mineralization rates and the total mineralization fraction were positively correlated with the initial phenanthrene bioavailability, assessed via β-HPCD extraction. Phenanthrene exposure induced significant responses of the catabolic gene biomarker *nidA*, fungi and bacteria communities by 275, 30, and 5 times, respectively, indicating a non-neglectable role of the fungal communities in phenanthrene mineralization. CNMs exerted a sorption- and level-dependent suppression (7.4–47.2%) on the total phenanthrene mineralization fractions at 120 d. Carbon nanotubes (300, 3000 mg/kg) caused significant adverse effects on the biomass of bacterial (47.8–60.7%), fungal (31.4–71.6%) and *nidA*-carrying degraders (25.7–59.9%) in the absence or presence of phenanthrene, which contributed to the inhibition of the total mineralization fractions at 120 d. Bacterial community structure was not significantly impacted by CNMs alone or co-exposure of CNM-phenanthrene. However, the fungal community showed a significant shift upon exposure to carbon nanotubes, especially M8, with the relative abundance of potential PAH degraders repressed (8.5–40.3%) at both levels of M8 tested. This corroborates the higher sensitivity of fungal communities. The findings from this study are important to inform how the released CNMs affect soil microbial communities that play a key role in the fate and remediation of organic contaminants in soil.

1. Introduction

Soil is an important sink for many persistent organic contaminants such as polycyclic aromatic hydrocarbons (PAHs). Microorganisms play an important role in PAH attenuation in soil, which is a highly complex system enriched in a considerable diversity of microbial communities (Vinas et al., 2005). The PAH ring-hydroxylating dioxygenase (PAH-RHD) initiates the aerobic degradation of PAHs. The genes (PAH-RHD$_\alpha$) encoding the large α subunit of this enzyme have been widely used as biomarkers for assessing the PAH-degradation potential in soils and sediments (Ding et al., 2010; Jurelevicius et al., 2012; Xia et al., 2015). Debruyn et al. (2007) found a significantly positive correlation between the *nidA* gene and pyrene degradation. Although bacteria are assumed to play a dominant role in hydrocarbon degradation especially in marine ecosystems, fungi were shown to be more important in freshwater and terrestrial environments (Olajire and Essien, 2014; Salvo et al., 2005). A group of fungi within *Ascomycota*, such as genera *Aspergillus*, *Pensillium*, *Cephalosporium* and *Fusarium* are capable of degrading crude oil and aromatic hydrocarbons (Singh, 2006). Winquist et al. (2014) found that the fungal community responded more rapidly to the presence of benzo[*a*]pyrene than the bacterial community, reflecting non-specific nature of fungal PAH degradation.

Abbreviation: CNMs, Carbon nanomaterials; M8 and M50, multi-walled carbon nanotubes with outer diameter < 8 nm and > 50 nm

* Corresponding author.
E-mail address: xilong@pku.edu.cn (X. Wang).

https://doi.org/10.1016/j.impact.2018.08.001
Received 11 April 2018; Received in revised form 20 July 2018; Accepted 1 August 2018
Available online 02 August 2018

The rapid development of nanotechnology has increased the likelihood of accidental and incidental release of nanomaterials to the environment, especially reaching soil systems that serves as a main receptor of these materials. The presence of carbon-based nanomaterials (CNMs) in soil may strongly affect the bioavailability of PAHs to soil microorganisms, due to their high affinity and sorption capacity for such hydrophobic organic contaminants (Wang et al., 2010; Yang et al., 2006), which would impact their biodegradation by indigenous microorganisms. The effects of CNMs on microbial bioavailability of organic contaminants have been widely studied (Cui et al., 2011; Towell et al., 2011; Xia et al., 2010; Xia et al., 2013; Yang et al., 2017; Zhang et al., 2016; Zhu et al., 2016; Oyelami and Semple, 2015), but data on how CNMs affect PAH mineralization kinetics are scarce. Zhou et al. (2013) found a significant inhibition of ^{14}C-2,4-dichlorophenol mineralization by 13.9% and 10.2% in the presence of 2000 mg/kg single-walled and multi-walled carbon nanotubes (SWCNTs and MWCNTs), respectively, in a rice paddy soil. Shan et al. (2015) also reported that the mineralization of ^{14}C-catechol in an agricultural soil was significantly reduced by 16.5–17.7% and 19.2% with activated carbon at all levels tested (0.2, 20, 2000 mg/kg) and SWCNTs at 2000 mg/kg, respectively, but was stimulated (19.0%) in the case of 0.2 mg/kg MWCNTs. However, the specific pollutant degraders and functional genes affected by CNMs were not identified.

Although bioavailability of organic contaminants is important for biodegradation, knowledge regarding the biomass and structure of specific microbial communities can provide a first glance at degradation potential and the physiological mechanisms that might impact degradation (Kostka et al., 2011). Antimicrobial properties of CNMs in culture conditions has been observed in many previous studies (Bai et al., 2011; Rodrigues and Elimelech, 2010; Liu et al., 2009; Jin et al., 2013). However, much less is known about their effects on indigenous microorganisms in the complex and real soil environment, especially for the fungal community and potential degraders. For instance, Chung et al. (2011) observed a significant inhibition of the microbial biomass C and enzymatic activities upon exposure to 5000 mg/kg MWCNTs after 20 d. As for the graphene oxide with more hydrophilic functional groups than carbon nanotubes, no significant suppression effect on biomass C was observed at 500–1000 mg/kg throughout the 59 d incubation (Chung et al., 2015). No significant effect of MWCNTs was observed at a concentration up to 2000 mg/kg on soil microbial biomass C after 61 d incubation (Shan et al., 2015), but the same concentration of single-walled carbon nanotubes resulted in a significant repression of microbial biomass C and a significant shift in microbial communities. These divergent observations could reflect differences in specific CNM and soil properties, microbial communities and exposure conditions.

Overall, information on how CNMs affect the mineralization patterns of organic contaminants by soil indigenous microorganisms is scarce and the underlying mechanisms are not fully understood. Most previous studies are constrained to short-term effects under scenarios not representing plausible exposure scenarios. In this work, we quantify copy numbers of the 16S rRNA, 18S rRNA and *nidA* genes in soil as affected by CNMs alone and CNM-contaminant co-exposure to gain mechanistic insight on the effects of CNM co-exposure on PAH mineralization kinetics. Bacterial and fungal community structures were also determined before and after exposure using a high-throughput sequencing technique. Findings from this study are important for evaluating how the fate and risk of organic contaminants might be affected by CNMs in soil, which informs both risk assessment of CNMs to microbial ecosystem services and bioremediation of hydrophobic organic pollutants.

2. Materials and methods

2.1. Chemicals

^{14}C-phenanthrene (≥ 98% radiochemical purity; 55 mCi/mmol) was purchased from Moravek Biochemicals Co. Ltd., USA, and non-labeled phenanthrene (> 98% purity) was obtained from AccuStandard Chemical Ltd., USA. Hydroxypropyl-β-cyclodextrin (β-HPCD, ≥ 97% purity) and the organic solvents including *n*-hexane, acetone and acetonitrile of HPLC grade were purchased from J&K Scientific, USA. The multi-walled carbon nanotubes (MWCNTs) with outer diameter < 8 nm (M8, > 95% purity) and > 50 nm (M50, > 95% purity) were purchased from Chengdu Organic Chemicals Co. Ltd., Chinese Academy of Sciences. C_{60} fullerenes with purity > 99% was provided by the Yongxin Fullerene Company in Henan Province, China. Selected physicochemical properties of carbon nanomaterials are summarized in Table S1 and the detailed characterization methods are described in the supporting information. Morphology of the nanomaterials was observed using transmission electron microscopy (Fig. S1). Sorption isotherms of phenanthrene towards soil and the CNMs were obtained using batch experiments with the initial sorbate concentrations ranging in 10–90% of its water solubility. The detailed information is described in SI. Sorption data were fitted with the logarithmic form of Freundlich model and the isotherms and parameters are presented in Fig. S2 and Table S2.

2.2. Soil

A clay loam (sand: 50.13%, silt: 26.28%, and clay: 23.59%) with pH of 6.63 and cation exchange capacity (CEC) of 41.88 cmol/kg was collected from a forest land in Dehui, Jilin Province, China, with an organic matter (OM) content of 321.63 g/kg and total organic carbon (TOC) content of 10.31% (Wang et al., 2016). The background concentration of phenanthrene was 121.81 μg/kg as reported in our recent study (Zhang et al., 2017).

2.3. Mineralization

Mineralization of ^{14}C-phenanthrene was investigated using a respirometer as described in our previous study (Yang et al., 2010). Briefly, the respirometer was made by attaching a 2.0-mL GC vial under the screw cap of a 40 mL amber vial. The GC vial was filled with 1.5 mL of 1 M NaOH solution to capture the $^{14}CO_2$ mineralized by the indigenous microorganisms in soil. Five grams of the air-dried soil were added to 40 mL amber vials, and then spiked with 100 μL non-labeled phenanthrene dissolved in acetone (1000 mg/L). Here, acetone was chosen as the solvent because it is readily evaporated and is mutually dissolvable with methanol where ^{14}C-phenanthrene is dissolved. The same solvent was used for the incubation conducted in Section 2.4. The initial non-labeled phenanthrene concentration in soil was 18.5 mg/kg. Twenty microliters of ^{14}C-phenanthrene (9.34 mg/L, 0.107 MBq/mL) dissolved in methanol were amended to the vial using a microsyringe to yield a radioactivity of 0.0115 μCi/g dry soil; the chemical concentration of ^{14}C-phenanthrene was 0.037 mg/kg dry soil. The vials were opened and placed in a fume hood for 0.5 h to evaporate the solvent, and then sealed and thoroughly mixed on a rotary shaker at 45 rpm for 72 h. For the mineralization test systems in which CNMs were added, the soil was initially spiked with non-labeled and labeled phenanthrene, thoroughly mixed as described above and then amended with C_{60}, M50, or M8 in dry powder form at concentrations of 300 and 3000 mg/kg dry soil. These two amendment levels likely appear in some “hot spots” where these materials are enriched. Furthermore, the low amendment level was below the most frequently administrated concentrations in the literature (550 mg/kg) and that of 3000 mg/kg was amended as for the comparison with other relevant studies (Ferguson et al., 2008; Shen et al., 2012; Petersen et al., 2009; Holden et al., 2014; Towell et al.,

2011; Oyelami and Semple, 2015; Chung et al., 2011). The bottles were sealed again and homogenized for 72 h using the same rotary shaker. ^{13}C-MWCNT was used to determine the uniformity of MWCNTs in soil, and the standard deviation of their concentrations was tested to be < 7% of the mean value (n = 6, Table S3). After homogenization, the soil was moistened with 2 mL sterilized Milli-Q water and equilibrated for 12 h, and then stirred with a stainless-steel spatula. All respirometers were run in triplicate and were incubated in a chamber in the dark at 25 °C with 60% relative humidity. At 1, 4, 8, 14, 20, 28, 35, 45, 60, 90, 120 d, the NaOH solution was sampled and mixed with 4 mL cocktail before radioactivity measurement with a liquid scintillation counter (LSC, LS 6500, Beckman Coulter, USA). The mineralization percentage of phenanthrene was calculated as a ratio of the radioactivity of $^{14}CO_2$ to that of the total ^{14}C in soil. Approximately 0.5 g dry soil was combusted at 900 °C in a biological oxidizer (OX-500; Zinsser Analytic, Germany) to determine the initial total ^{14}C radioactivity. The $^{14}CO_2$ was absorbed by 15 mL of alkaline cocktail Oxysolve C-400 (Zinsser Analytic, Germany) and the radioactivity was determined using LSC. The NaOH-captured ^{14}C radioactivity in sterilized soil was also measured so as to monitor the possible evaporation of this compound during 120 d incubation; the results showed that the ^{14}C radioactivity values were all below 20 dpm throughout the whole period, which excluded the bias from ^{14}C-phenanthrene evaporation. A conceptual model describing the interactions between individual components in the CNMs exposure systems is displayed as Fig. S3 in SI.

2.4. The total and mildly extracted phenanthrene from soil

To evaluate the impact of CNMs on the total and bioavailable fractions of phenanthrene during the 120 d exposure, various treatments with non-labeled phenanthrene and/or CNMs were simultaneously conducted. One hundred air-dried soil was added to 250 mL bottles and then amended with 400 μL of phenanthrene solution (5000 mg/L) dissolved in acetone. After the solvent was evaporated in a fume hood for 4 h, the bottle was sealed and vigorously shaken on a rotary shaker at 45 rpm for 72 h. Treatments amended with CNMs were prepared the same way as described in Section 2.3. After homogenization, the soil was transferred to a 250 mL jar and moistened with 40 mL sterilized Milli-Q water to reach an approximately 60% of the maximal water-holding capacity; CNMs at both 300 and 3000 mg/kg did not significantly change the water holding capacity of soil (Table S4). The soils were equilibrated for about 12 h, and then stirred with a stainless-steel spatula. After 1, 4, 8, 14, 20, 28, 35, 45, 60, 90, 120 d, fresh soil was sampled from the top, middle and bottom of each container and mixed; the total and mildly extracted fractions were measured following the procedure in our recent study (Zhang et al., 2017). The total phenanthrene was extracted with 1:1 (v:v) hexane/acetone and then cleaned up on a silica solid phase extraction column (CNW); the bioavailable fraction was extracted using β-HPCD. The phenanthrene concentration in all samples was analyzed with HPLC equipped with a UV-detector (Agilent 1100 Series). Detailed sample preparation and chemical analysis are described in SI. Both the total and bioavailable phenanthrene fractions in soil (including that at 12 h equilibrium shown as "0" d) were calculated as a percentage of the initial concentration determined before moistened.

2.5. Microbial biomass C

Microbial biomass carbon was determined using the chloroform fumigation extraction method (Vance et al., 1987). Briefly, at the end of 120 d incubation in Section 2.4, 5 g of fresh soil was sampled from each container and was fumigated with ethanol-free chloroform in a vacuum desiccator in the dark for 24 h. The non-fumigated and fumigated soils were extracted with 20 mL of 0.5 M K_2SO_4 on a rotary shaker for 30 min and then filtered. The filtrate was analyzed for its total organic carbon concentration using a TOC analyzer (Shimadzu TOC5000a). The microbial biomass C was calculated using the following equation:

$$\text{Biomass C} = \frac{E_c}{0.45}$$

where E_c is the difference between TOC extracted from fumigated and non-fumigated soil. The value of 0.45 is a coefficient between biomass C and E_c (Vance et al., 1987). The microbial biomass C is expressed as mg C/kg soil.

2.6. Soil DNA extraction, PCR amplification and sequencing

After 120 d incubation, triplicate portions of the total DNA in the fresh soil (approximately 0.5 g) from various treatments was extracted using a PowerSoil DNA extraction kit (Mo Bio Laboratories, Inc., Carlsbad, CA) following the manufacturer's instructions. The final concentration and purity of DNA were determined using a NanoDrop 2000 UV–vis spectrophotometer (ThermoFisher Scientific, Wilmington, USA). The DNA quality was tested by 1% agarose gel electrophoresis with a voltage at 5 V/cm for 30 min. The universal primers 515F (GTGCCAGCMGCCGCGG) and 907R (CCGTCAATTCMTTTRAGTTT) were used for amplification of the V4 region of 16S rRNA genes. Primers for 18S rRNA genes were SSU0817F (TTAGCATGGAATAATRRAATAGGA) and 1196R (TCTGGACCTGGTGAGTTTCC). PCR amplification for 16S rRNA and 18S rRNA was performed in triplicate in a 20-μL mixture containing 4 μL of 5 × PastPfu Buffer (TransGen, Beijing), 2 μL of 2.5 mM dNTPs, 0.8 μL of each primer (5 μM), 0.2 μL of Bovine serum albumin, 0.4 μL of TransStart FastPfu DNA Polymerase and 10 ng of template DNA. The PCR reaction and the subsequent purification are described in SI.

Raw fastq files were demultiplexed, quality-filtered by Trimmomatic and merged by FLASH with the following criteria: (1) The reads were truncated at any site receiving an average quality score < 20 over a 50 bp sliding window; (2) Primers were exactly matched allowing two nucleotide mismatching, and reads containing ambiguous bases were removed; (3) Sequences with overlap longer than 10 bp were merged according to the overlap sequence. Operational taxonomic units (OTUs) were clustered with 97% similarity cutoff using UPARSE (version 7.1) and chimeric sequences were identified and removed using UCHIME. The taxonomy of each 16S rRNA and 18S rRNA gene sequence was analyzed by RDP Classifier algorithm against the Silva (SSU123) 16S rRNA database and Silva (SSU123) 18S rRNA database using confidence threshold of 70%.

2.7. qPCR

As a proxy for specific microbial biomass, the copy numbers of 16S rRNA, 18S rRNA and PAH-RHD$_\alpha$ genes were determined using qPCR. The *nidA* gene was amplified using primers *nidA*F (TTCCCGAGTACGAGGGATAC) and *nidA*R (TCACGTTGATGAACGACAAA) according to Debruyn et al. (2007). qPCR was performed in triplicate using a real-time PCR system LineGene 9600 Plus (Bioer Techology Co., Ltd., China). qPCR for 16S rRNA, 18S rRNA, and *nidA* genes was performed in a 20-μL reaction mixture containing 10 μL of 2 × SYBR Mixture (with ROX) (UPTECH Life Science, China), 0.4 μL of each primer (10 μM), 1 μL of DNA, and 8.2 μL of RNase-Free ddH_2O. The detailed qPCR procedure is described in SI. Tenfold serial dilutions of PUC-T plasmid (CWBIO, China) containing a PCR fragment amplified from the *Escherichia coli* DH5$_\alpha$ genes (CWBIO, China) were used to establish the standard curves. Standard stock solutions of 3.06×10^8, 2.9×10^8 and 3.22×10^8 copies/μL were prepared for 16S rRNA, 18S rRNA and *nidA* genes, respectively.

2.8. Data analysis

Phenanthrene mineralization data were fitted with the logistic growth equation as follows:

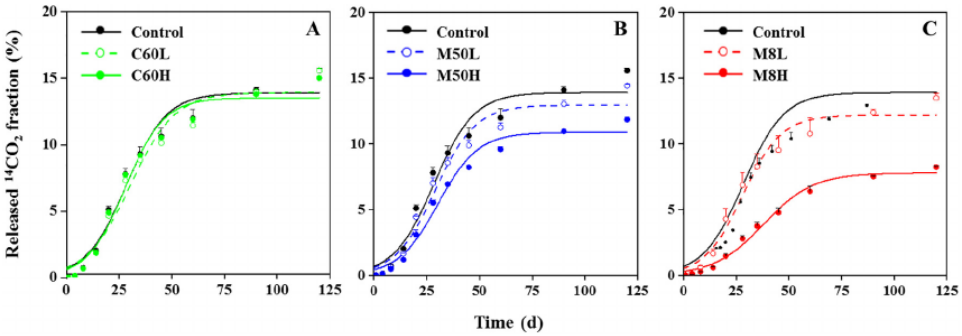

Fig. 1. Mineralization fraction (released $^{14}CO_2$) from ^{14}C-phenanthrene by soil indigenous microbial communities as affected by C_{60} (A), M50 (B) and M8 (C) during 120 d incubation. "Control" indicates soil spiked with phenanthrene alone. C_{60}L, M50L, and M8L indicate soil amended with phenanthrene and 300 mg/kg of these nanomaterials; C_{60}H, M50H and M8H refer to soil amended with phenanthrene and 3000 mg/kg of these nanomaterials.

$$M_f = \frac{a}{1 + e^{-\left(\frac{t-t_0}{b}\right)}}$$

where M_f is the mineralization fraction (%); a is the maximum mineralization fraction (%); t is the time (d); t_0 is the time when half the maximum mineralization fraction is reached (d); b is a parameter indicating acclimation of the microorganisms (d). Statistical significance was determined using a one-way ANOVA with a Tukey's multiple comparison test in SPSS 20.0 (IBM Analytics). Differences were considered significant at $p < 0.05$.

3. Results and discussion

3.1. Mineralization kinetics and microbial response in phenanthrene-spiked soil

The mineralization kinetics of phenanthrene by indigenous microorganisms was fitted well with the logistic growth equation ($R^2 = 0.969$, Fig. 1 and Table 1). Mineralization in CNM-free soil displayed an obvious lag phase (9.27 d) at the very beginning, indicating a growth and/or adaptation of soil microorganisms. In contrast, Shan et al. (2015) did not find such a lag phase during the mineralization of ^{14}C-catechol by indigenous microorganisms in an agriculture soil; the mineralization rate was the maximum at the beginning, followed by a slow decline until the end of 60 d exposure. At around 28 d, phenanthrene mineralization reached a maximum rate of 0.36% 1/d (Table 1). At the end of the 120 d exposure, the total mineralized fraction was 15.58% of the initial amount, indicating a limited mineralization of phenanthrene by the indigenous microorganism in this soil (Fig. 1). However, the degradation fraction of this compound could be greater because mineralization is the final step of the degradation, which involves both transformation and mineralization processes. Oyelami and Semple (2015) observed a much higher mineralization fraction of phenanthrene (47.8%) by the indigenous microorganisms in a pasture soil solution after 14 d incubation. In comparison, Shan et al. (2015) found 18.5% mineralization of ^{14}C-catechol by the microorganisms in an agricultural soil after 60 d exposure.

Notwithstanding the limited mineralization, a 4.8 times higher 16S rRNA gene abundance was detected in the phenanthrene-spiked soil relative to that in the clean soil (Fig. 2A), indicating a time integrated response of the bacterial communities. *Proteobacteria* was the most abundant phylum of the bacteria, accounting for 38.2% in the control soil, followed by *Actinobacteria* (17.3%) and *Acidobacteria* (13.4%) (Fig. 3A). Members of *Proteobacteria* contain many potential degraders of PAHs such as *Pseudomonas*, *Sphingomonas*, *Burkholderia*, *Ralstonia* and *Cycloclasticus* (Sawulski et al., 2014; Niepceron et al., 2010). However, these genera accounted for < 0.01% of the total community in both the clean and phenanthrene-spiked soil. *Actinobacteria* such as *Rhodococcus*, *Mycobacterium* and *Nocardia* have been found to degrade PAHs in pure culture and the environment (Walter et al., 1991; Boldrin et al., 1993; Moody et al., 2001; Zeinali et al., 2008), which were all below 0.4% of the total bacteria in the test soil. These observations may be associated with the limited mineralization fraction of phenanthrene as mentioned above.

In addition to the bacterial abundance, phenanthrene exposure also led to a significant shift in the bacterial structure after 120 d incubation (Fig. 3A); this was also reflected by the phenanthrene group that was distinctly separated from the control (Fig. 4A). Specifically, the relative abundance of *Proteobacteria* phylum was notably reduced by 18.5%, indicating an adverse effect of phenanthrene exposure. Within this phylum, the *Gammaproteobacteria* class was reduced by 61.2%, while those of *Beta-* and *Delta-proteobacteria* were increased to 1.7 and 1.4

Table 1
Kinetics parameters for the mineralization of phenanthrene by soil indigenous microorganisms

Treatments	a (%)	t_0 (d)	b (d)	Mineralization fraction (%)	MMR (% 1/d) [a]	Lag phase (d) [b]	R^2
Control	13.92 ± 0.37	28.43 ± 1.17	9.58 ± 0.88	15.58	0.36	9.27	0.969
C60L	13.95 ± 0.40	30.41 ± 1.30	10.52 ± 0.98	15.60	0.33	9.36	0.966
C60H	13.53 ± 0.32	27.93 ± 1.00	9.10 ± 0.76	15.02	0.37	10.87	0.975
M50L	12.95 ± 0.32	29.03 ± 1.07	9.51 ± 0.81	14.42	0.34	10.01	0.974
M50H	10.88 ± 0.22	30.36 ± 0.89	9.48 ± 0.68	11.85*	0.29*	11.40*	0.982
M8L	12.18 ± 0.34	28.10 ± 1.18	9.07 ± 0.90	13.49	0.34	9.95	0.965
M8H	7.80 ± 0.16	37.98 ± 1.01	11.80 ± 0.74	8.23**	0.17**	14.39**	0.985

C_{60}L, M50L, and M8L indicate soil amended with phenanthrene and 300 mg/kg of carbon nanomaterials.
C_{60}H, M50H and M8H refer to soil amended with phenanthrene and 3000 mg/kg of carbon nanomaterials.
Significant level: * ($p < 0.05$); ** ($p < 0.01$).
[a] MMR (maximum mineralization rate) was calculated based on the maximum slope of the tangent line.
[b] Lag phase was calculated as the intersection of x-axis with the tangent line at the point while the maximum degradation rate achieved (Broos et al., 2005).

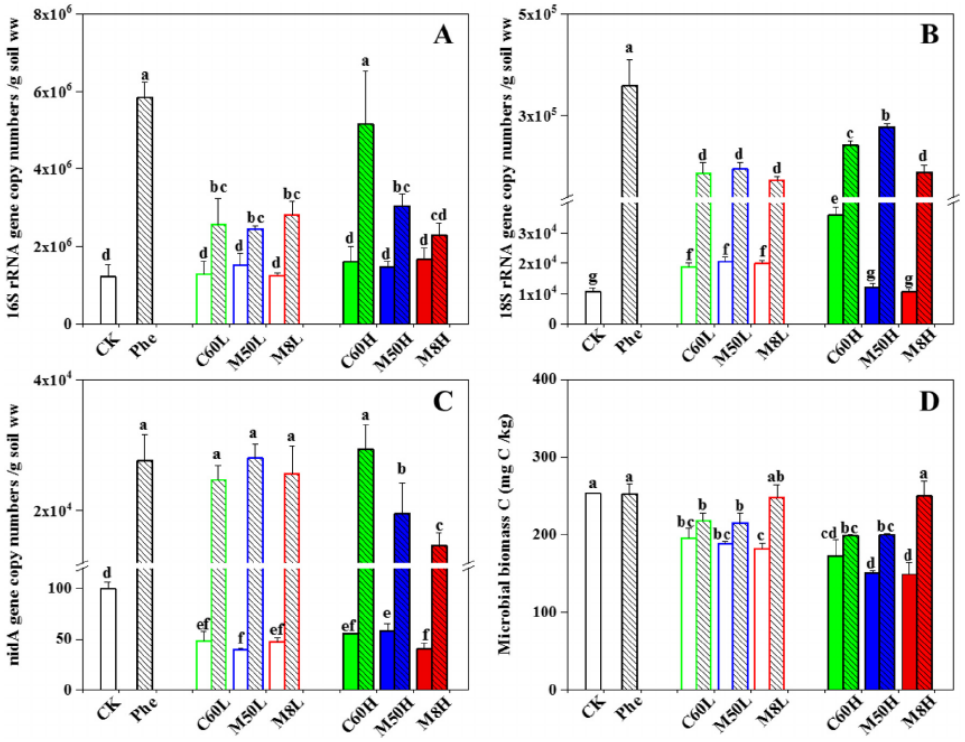

Fig. 2. Copy numbers of 16S rRNA (A), 18S rRNA (B) and *nidA* genes (C), as well as microbial biomass C (D) in soil under single and combined exposures of phenanthrene and CNMs after 120 d incubation. "CK" indicates soil without any amendment and "Phe" indicates that with phenanthrene alone. C60L, M50L and M8L means soil amended with 300 mg/kg CNMs; C60H, M50H, and M8H refer to soil amended with 3000 mg/kg CNMs. Hollow columns denote soil with CNMs alone, and those with slash shadows are soil amended with CNMs and phenanthrene. Column values marked with the same letter are not statistically different ($p < 0.05$).

times that the control (Fig. 3C). This observation was not in agreement with previous studies. For instance, Niepceron et al. (2013) observed an early and sustainable increase in *Gammaproteobacteria* relative abundance from a grassland soil spiked with a PAH mixture (300 mg/kg) from 30 d to the end of the incubation (90 d). The authors also detected a significantly higher relative abundance of *Betaproteobacteria* in this microcosm, but the increase occurred late after 60 d incubation and did not last long. The dissimilar responses from specific microbial communities could result from the types and concentrations of PAHs, as well as the distinct structure and abundance of soil microbial communities. Phyla *Actinobacteria* and *Acidobacteria* also have been found to play a significant role in PAH degradation (Sawulski et al., 2014), but a significant increase of 20.1% was only found for *Actinobacteria* upon phenanthrene exposure (Fig. 3A).

The 18S rRNA abundance was 30.1 times higher in the phenanthrene-spiked soil compared to that in the clean soil, indicating a more pronounced activity of the fungal community (Fig. 2B). It was reported that most of the pollutant degraders belong to the phyla *Ascomycota* and *Basidiomycota* (Harms et al., 2011; Singh, 2006).

In the present study, *Ascomycota* (89.1%) phylum was the most abundant in the control soil followed by *Basidiomycota* (3.1%) and *Amoebozoa* (2.5%), reflecting a degradation potential of the fungal community. No significant change in *Ascomycota* abundance was observed upon exposure to phenanthrene (Fig. 3B). However, within this phylum, the relative abundance of the class *Sordariomycetes* was increased to 3.0 times that the control (Fig. 3D), in which the unclassified genera belonging to order *Hypocreales* increased by 11.2 times and became the most dominant species (Fig. 3F). This order was reported to be associated with metabolization of polychlorinated dibenzo-p-dioxins (Harms et al., 2011). In contrast, members of the class *Leotiomycetes* were sharply decreased by 73.6% (Fig. 3D), accompanying with a significant adverse effect of phenanthrene exposure on the genus *Helotiales* within this class (Fig. 3F). The α-diversity of the fungal community showed a slight but insignificant decrease upon phenanthrene exposure, while that of the bacteria was comparable with the control (Tables S5 and S6).

As a gene encoding the α-subunit of the dioxygenase involving in the first step of PAH degradation, the copy number of *nidA* genes at 120 d was significantly enhanced by 275.3 times upon phenanthrene exposure (Fig. 2C). This indicated a positive response of the degraders to phenanthrene exposure, which in turn led to its mineralization in soil. However, as a sensitive indicator for early changes in the function of soil microbial community, the microbial biomass C at 120 d was not significantly affected by the phenanthrene exposure alone (Fig. 2D). This indicated little net effect on the growth of the overall microbial community at the end of exposure. It is most likely that the transit change in biomass C has occurred during the exposure period but finally recovered to the original state.

3.2. Mineralization kinetics influenced by CNMs

3.2.1. Lag phase, maximum mineralization rate and mineralization fraction

The mineralization dynamics of phenanthrene in the presence of CNMs was also fitted well with the logistic growth equation (R^2 = 0.965–0.985, Fig. 1 and Table 1). C_{60} did not significantly affect the lag phase at both amendment levels (Table 1). In comparison, carbon nanotubes resulted in longer lag phases, with significant increases being 1.2 and 1.6 times the control under the co-exposure of

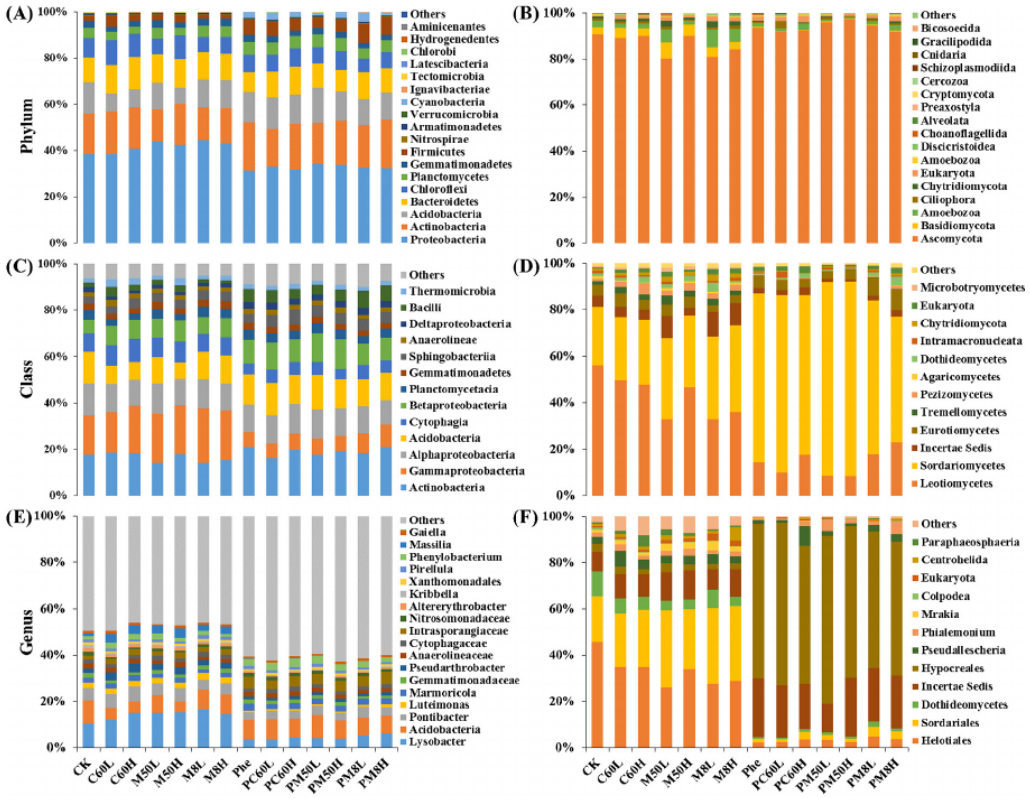

Fig. 3. Phylum- (A, B), Class- (C, D) and genus- (E, F) level communities of soil bacterial (A, C, E) and fungal (B, D, F) under single and combined exposures of phenanthrene and carbon nanomaterials (CNMs) after 120 d incubation. "CK" indicates soil without any amendment and "Phe" indicates that with phenanthrene alone. C60L, M50L, and M8L indicate soil amended with 300 mg/kg CNMs; C60H, M50H, and M8H indicate soil amended with 3000 mg/kg CNMs. PC60L, PM50L and PM8L indicate soil amended with phenanthrene and 300 mg/kg CNMs; PC60H, PM50H and PM8H indicate soil amended with phenanthrene and 3000 mg/kg CNMs. Bacteria phyla < 0.01%, as well as classes and genera < 1% were displayed as others. Fungal phyla < 0.01%, as well as classes and genera < 0.5% were displayed as others.

3000 mg/kg M50 and M8, respectively. Carbon nanotubes have sites at both interstitial and external surfaces for phenanthrene sorption, while the sorption sites for this compound by C_{60} are only limited to its external surfaces. As shown in Fig. S2 and Table S2, the surface areas of M50 and M8 were 44 and 222 times that of C_{60}; the K_d values of phenanthrene by M50 and M8 were 33 and 229 times that of C_{60},

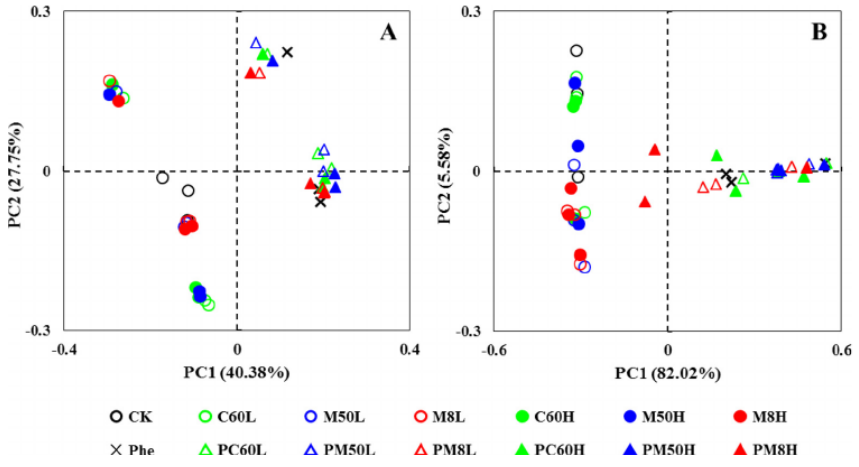

Fig. 4. Principal component analysis (PCA) of soil bacterial (A) and fungal (B) communities under various treatments after 120 d mineralization. "CK" indicates soil without any amendment and "Phe" refers to that with phenanthrene alone. C60L, M50L, and M8L indicate soil amended with 300 mg/kg CNMs; C60H, M50H, and M8H indicate soil amended with 3000 mg/kg CNMs. PC60L, PM50L and PM8L indicate soil amended with phenanthrene and 300 mg/kg CNMs; PC60H, PM50H and PM8H indicate soil amended with phenanthrene and 3000 mg/kg CNMs.

Table 2
Correlation between the mineralization rate (M_{rate}, %·1/d) of phenanthrene and the bioavailability (S_{bio}, %) or residual content (S_{res}, %) at the starting point of each time interval.

Time interval (d)			0–1	1–4	4–8	8–14	14–20	20–28	28–35	35–45	45–60	60–90	90–120
M_{rate}	S_{bio}	r	0.013	*0.750*	*0.857*	*0.766*	*0.819*	*0.859*	0.049	0.152	0.129	0.408	0.298
		p	0.965	*0.002*	*0.000*	*0.001*	*0.000*	*0.000*	0.868	0.604	0.661	0.148	0.301
		R^2	0.000	*0.564*	*0.734*	*0.587*	*0.670*	*0.737*	0.002	0.024	0.017	0.166	0.088
M_{rate}	S_{res}	r	0.000	*0.946*	*0.980*	*0.909*	*0.938*	*0.991*	*0.974*	*0.915*	*0.770*	*0.853*	*0.906*
		p	0.999	*0.001*	*0.000*	*0.005*	*0.002*	*0.000*	*0.000*	*0.004*	*0.043*	*0.015*	*0.005*
		R^2	0.000	*0.893*	*0.960*	*0.827*	*0.879*	*0.982*	*0.949*	*0.838*	*0.593*	*0.726*	*0.821*

r is Pearson correlation coefficient; Significant correlations are in italic.

respectively. Lag phases under a high level of CNMs exhibited an order of C_{60} < M50 < M8, which was consistent with the sorption strength. Lag phases from all treatments displayed a significantly negative correlation with the initial bioavailability (Pearson correlation coefficient r = −0.882, significance level p = 0.009), suggesting a faster acclimation of the microorganisms in the case with a higher bioavailability of phenanthrene. The initial bioavailable phenanthrene in soil (indicated as "0 d" in Fig. S4, A) accounted for 15.1–31.0% of the total concentration in the absence and presence of CNMs. The compound bioavailability decreased fast in the initial few days, followed by a relatively slow decline to < 6% after 120 d. A significant increase (11.4–12.9%) in contaminant bioavailability was observed upon exposure to 3000 mg/kg C_{60} during the first 14 d. The K_d values of phenanthrene by C_{60}, M50, and M8 were 2, 75, and 517 times that by soil, respectively (Fig. S2, Table S2). As such, once water was added to soil, the contaminant would transfer from the soil matrix to the amended carbon nanomaterials. In this process, the phenanthrene fraction in porewater may be higher than the soil without any amendment. Besides, phenanthrene sorbed on soil-C_{60} mixture with slightly greater sorption strength may not be recalcitrant to be extracted by β-HPCD, thus increasing the apparent bioavailable fraction. In contrast, carbon nanotubes having much higher sorption strength for phenanthrene significantly reduced phenanthrene bioavailability during the first 14–20 d, especially for M8. However, after 28 d, the differences in contaminant bioavailability were not significant among all treatments and the control, which may be attributed to the rather low bioavailable fractions after this time point (Zhang et al., 2017). On the contrary, a positive correlation was observed between the lag phase and the initial residual contents (r = 0.936, p = 0.002); this indicated that the microorganisms need a long adaptation when the total phenanthrene concentration is high, which probably is associated with the high toxicity to the microbes.

The maximum mineralization rates (MMR) reached at 27.87–37.96 d for various CNM treatments. Both levels of C_{60}, as well as the low level of M50 and M8 had little effect on MMR compared to the control (Table 1). However, a high level of M50 and M8 exhibited a significant suppression on the MMR by 20.9% and 54.5%, respectively. The MMR obtained from the control and CNM treatments was positively correlated with the corresponding initial bioavailability (r = 0.969, p = 0.000) and negatively correlated with the initial residual contents (r = −0.975, p = 0.000). Although the bioavailability during the later phase of exposure was comparable under various CNM treatments, the initial bioavailability was a potential factor impacting the lag phase and MMR of contaminant by soil indigenous microorganisms. This suggested a possible prediction of the mineralization kinetics under certain CNM treatments according to the initial bioavailability and residual contents of phenanthrene in soil.

CNMs resulted in varying effects on the total mineralization fraction of phenanthrene, ranging from 8.23–15.60%. Specifically, C_{60} at both 300 and 3000 mg/kg exhibited insignificant effect on the total mineralization fraction of phenanthrene after 120 d (Fig. 1A), indicating little effect on the degradation activity. This was in agreement with the findings by Oyelami and Semple (2015) that phenanthrene mineralization was not significantly affected by the co-exposed C_{60} at concentrations ranging from 0.01 to 1%. In comparison, MWCNTs exhibited a level-dependent suppression on the 120-d mineralization fraction. For instance, the mineralization fractions were 7.4% and 23.9% (M50), as well as 13.4% and 47.2% (M8) lower than the control at 300 and 3000 mg/kg, respectively. However, the effect was only significant at the high amendment level (Fig. 1B, C). As the CNMs were amended at a certain level, the mineralization fraction displayed an order of C_{60} > M50 > M8, which was opposite to their sorption strength. This indicated an important role of bioavailability in mineralization of phenanthrene by indigenous microorganisms, especially in the treatment with carbon nanotubes possessing greater sorption strength than C_{60} and soil matrix. Specifically, the K_d values (at 0.1 S_w) by M50 and M8 were 75 and 517 times that by soil, and were 33 and 229 times that by C_{60}, respectively (Fig. S2, Table S2). A significant positive correlation was observed between the total mineralization fraction and the initial bioavailability of phenanthrene (r = 0.954, p = 0.001). The total mineralization fraction was also significantly negatively correlated with the initial residual contents (r = −0.943, p = 0.001).

3.2.2. Time-dependent mineralization rate

To understand the mineralization rate of phenanthrene at each sampling point, the incubation period was divided into various time intervals as shown in Table 2. The correlation with bioavailability (M_{rate} S_{bio}) was significant for the time intervals from 1 to 28 d (r = 0.750–0.859, p = 0–0.002). However, this correlation was not significant after 28 d, which was due to the comparable bioavailability among CNM treatments after this time point (Fig. S4, A). Therefore, the mineralization rate was significantly dependent on the bioavailability during early exposure period but was not related to it after 28 d. However, the mineralization rate in each time interval was negatively correlated with the soil residual contents (r from −0.853 to −0.980, p = 0–0.043) except for 0–1 d. Although the soil amended with M50 and M8 resulted in 1.6–6.2 times higher residual contents of phenanthrene (Fig. S4, B), most of them could not be readily mineralized by the indigenous microorganisms. Based on above, in the presence of CNMs, bioavailability is an effective indicator for the initial mineralization rate but lost its role as the compound interacted with soil for a longer time. However, the residual contents performed very well in the prediction of mineralization rate for several months.

3.2.3. Community-specific effect on the total mineralization fraction

In addition to the role of bioavailability in mineralization, the activity and function of microbial communities also matter to the process. As mentioned in Section 3.1, microbial communities showed a significant response to the phenanthrene exposure alone, which is also an important indicator for the mineralization process as affected by the exposure to CNMs. CNMs may pose negative or positive effect on microbial communities resulting from CNMs alone and/or CNM-phenanthrene complex. Specifically, CNMs on their own resulted in a significant suppression on the microbial biomass C (Fig. 2D), indicating adverse effects on the microbial growth. In addition, the suppression

effect was more significant at a higher level of a certain CNM; reductions of microbial biomass C were 22.8%, 31.6%, and 25.4%, as well as 40.4%, 28.2% and 41.1% for the co-exposure to 300 and 3000 mg/kg C_{60}, M50 and M8, respectively. As for a given amendment level, the microbial biomass C followed the order of C_{60} > M50 > M8, which was reverse to the sorption strength of CNMs (Fig. S2 and Table S2). Jin et al. (2013) found a significant negative correlation between the microbial biomass C and N with the surface area of carbon nanotubes in an urban soil. The suppression effect in our results may stem from greater microorganism-CNT interactions or the alteration of soil structure and/or physicochemical properties (Jin et al., 2013; Shan et al., 2015). Furthermore, the communities carrying *nidA* gene were also significantly inhibited by 42.1–59.9% under all CNM exposures (Fig. 2C), but no differences were observed among these treatments, reflecting a dissimilar mechanism compared to that on the total microbial biomass. Nevertheless, these observations suggested a negative effect of CNMs on the overall microbial communities and the PAH degraders, which may have inhibited the total mineralization fraction of phenanthrene, especially for the case with carbon nanotubes. C_{60} at both levels exhibited a significant suppression on the microbial biomass C (Fig. 2D), which was not in agreement with other studies showing limited effects of C_{60} on soil microbial communities (Tong et al., 2007; Nyberg et al., 2008). With respect to the specific community, the 16S rRNA gene abundance was not significantly impacted by CNMs on their own, reflecting little effect on the bacterial biomass after 120 d incubation (Fig. 2A). It is possible that the bacterial communities recovered from the CNM effect during the long-term exposure. Ren et al. (2015) investigated the effect of graphene (10–1000 mg/kg) on the 16S rRNA copy numbers in a paddy soil. They only found a transient increase (after 4 d incubation) in the gene abundance under 100 mg/kg graphene, with the other treatments exhibiting no significant effect throughout the 60 d incubation. Rodrigues et al. (2012) observed a transient and adverse effect of carboxyl-functionalized SWCNTs (up to 500 mg/kg) on the number of bacterial colony-forming units (CFU) in 3 days, but a nearly full recovery in 7–14 days; however, fungal community did not recover from the dose-dependent suppression of the SWCNTs. In this study, the fungal biomass (18S rRNA gene copy numbers per gram soil) was significantly stimulated under the amendment of 300 mg/kg CNMs and 3000 mg/kg C_{60}, which was 1.7–3.3 times that of the blank soil (Fig. 2B). This again indicated a sorption-dependent role of CNMs in the growth of fungal community as observed in the case with microbial biomass C. The discrepancies among bacterial, fungal and *nidA* abundances in this study suggested a community-specific response towards the exposure of CNMs, which was associated with the dissimilar interactions between these communities and CNMs.

Co-exposure of phenanthrene with CNMs also resulted in varying effects on the biomass of specific microbial communities as compared to the case with phenanthrene alone (Fig. 2). The biomass C of the total community exhibited a level-dependent decrease under the co-exposure of C_{60} and M50 (Fig. 2D). For instance, C_{60} at 300 and 3000 mg/kg significantly decreased the microbial biomass C by 13.5% and 21.4%, respectively; co-exposure with M50 also reduced it by 14.9% and 21.0% at 300 and 3000 mg/kg, respectively. In comparison, M8 at both levels exhibited comparable microbial biomass C to that with phenanthrene alone, suggesting little net effect on the total microbial community. Co-exposure of phenanthrene with 300 mg/kg CNMs significantly reduced 16S rRNA and 18S rRNA gene abundance by 51.8–58.0% and 63.4–71.6% as compared to the case with phenanthrene alone (Fig. 2A, B). However, there were no significant differences among the CNMs. In comparison, the *nidA* abundance was not changed by the co-exposure to 300 mg/kg CNMs (Fig. 2C), which was consistent with the comparable mineralization fraction in these treatments. As the CNM level was increased to 3000 mg/kg, the abundances of 16S rRNA and *nidA* genes showed a similar trend of C_{60} > M50 > M8, with the C_{60} at this level showing no significant effects compared to those with phenanthrene alone (Fig. 2A, C). As for fungi, CNMs at 3000 mg/kg also led to significant reductions in its abundance by 31.4–65.7%, but showed a different trend of M50 > C_{60} > M8 (Fig. 2B). Overall, the microbial communities subjected to CNMs between the case with and without phenanthrene are dissimilar, which in turn reflected the microbial structure shift upon phenanthrene exposure alone. A high level of carbon nanotubes exerted negative effects on the biomass of bacterial, fungal and *nidA*-carrying communities, which made it a possible reason for the inhibition of mineralization in these cases.

3.2.4. Total mineralization fraction associated with microbial structure

The amendment of CNMs on their own at both low and high levels did not result in a significant effect on the bacterial composition after 120 d incubation (Fig. 3), as reflected by the convergence of these treatments (Fig. 4A). Similarly, as the CNMs were co-exposed with phenanthrene, the treatment groups also displayed a close distance from that with phenanthrene alone (Fig. 4A). In addition, the diversity indices in all these treatments were comparable with that of the control (Table S5). Carbon nanotubes on their own tended to increase the relative abundance of *Proteobacteria* (Fig. 3A), which contain many PAH degraders. This indicated that the mineralization inhibition from carbon nanotubes may not stem from their impact on this phylum. Within this phylum, the relative abundance of *Gammaproteobacteria* class and the genus *Lysobacter* belonging to this class generally exhibited a trend of C_{60} < M50 < M8 at a certain amendment level, regardless of the presence of phenanthrene (Fig. 3C, E). *Lysobacter* lack flagella but are highly mobile via a gliding mechanism; the exact function of this genus is unclear, but they are known to produce extracellular enzymes to cope with environmental stresses (Kobayashi and Crouch, 2009; Tong et al., 2012). In this study, the amendment of M8 did not inhibit but tended to increase the relative abundance of *Lysobacter* (Fig. 3E), which was the dominant species in the test soil, suggesting little adverse effect on this genus that might involve in the phenanthrene mineralization.

Different from bacteria, carbon nanotubes on their own led to a significant shift in the composition of fungal community, especially for M8 (Figs. 3 and 4B). Particularly, M8 significantly decreased the *Ascomycota* relative abundance by 11.8% and 8.5% at 300 and 3000 mg/kg, respectively; only 300 mg/kg M50 resulted in a decrease of 13.7% (Fig. 3B). C_{60} at both levels and M50 at a high level exhibited little effect on the fungal composition, but significantly reduced its α-diversity as shown in Table S6. Overall, all CNMs on their own exerted a negative effect either on the relative abundance of the potential degraders or the diversity of fungal community, which may lead to the inhibition of mineralization process. In comparison, co-exposure of CNMs with phenanthrene did not significantly alter the fungal composition compared to that exposed to phenanthrene alone, with these treatments clustered together as shown in Fig. 4B. Different from our observations, Ge et al. (2016) found a significant shift in bacterial communities by 1000 mg/kg of narrow MWCNTs (outer diameter < 8 nm) and graphene after 1-year exposure, but no such change was observed for the fungal communities. As for the soil planted with soybeans, Ge et al. (2018) observed a significant alteration of prokaryotic communities at the reproductive stage under the amendment of 0.1–1000 mg/kg MWCNTs and graphene with an exception of the highest level of MWCNTs, while that at the vegetative stage was only changed by 0.1 mg/kg MWCNTs. The discrepant findings largely resulted from the dissimilar carbon nanomaterials, microbial communities, exposure duration and conditions.

4. Conclusions

Phenanthrene mineralization in the nature soil was limited, but the exposure did induce a significantly positive response of the microbial communities, underlining a selective microbial shift and a promising degrader isolation where low contaminant mineralization is observed.

As contaminants usually weather to varying extents in the real environment, the contaminant bioavailability may not be an effective indicator for its mineralization rate. Carbon nanotubes released to the environment has a negative effect on the abundance of bacterial, fungal and nidA-carrying communities, which likely poses a threat to the function of these communities. M8 significantly inhibited the potential fungal degraders and had significant effect on PAH mineralization in the soil deposited with this nanomaterial. More attention in future studies should be paid to the role of indigenous fungal communities in the mineralization and degradation of organic contaminants.

Con icts of interest

There are no conflicts of interest to declare.

Acknowledgment

This study was supported by the National Science Fund for Distinguished Young Scientist (41525005), the 973 Program (2014CB441104), National Natural Science Foundation of China (41390240 and 41629101), and the 111 Program (B14001). We appreciated Professor Rong Ji at Nanjing University for the ^{14}C analysis. We also thank Dr. Yini Ma, Kun Lu and Chi Huang for the assistance with ^{14}C analysis.

Appendix A. Supplementary data

Supplementary data to this article can be found online at https://doi.org/10.1016/j.impact.2018.08.001.

References

Bai, Y., Park, I.S., Lee, S.J., Bae, T.S., Watari, F., Uo, M., Lee, M.H., 2011. Aqueous dispersion of surfactant-modified multiwalled carbon nanotubes and their application as an antibacterial agent. Carbon 49, 3663–3671.

Boldrin, B., Tiehm, A., Fritzche, C., 1993. Degradation of phenanthrene, fluorene, fluoranthene, and pyrene by a *Mycobacterium* sp. Appl. Environ. Microbiol. 59, 1927–1930.

Broos, K., Mertens, J., Smolders, E., 2005. Toxicity of heavy metals in soil assessed with various soil microbial and plant growth assays: as comparative study. Environ. Toxicol. Chem. 24, 634–640.

Chung, H., Son, Y., Yoon, T.K., Kim, S., Kim, W., 2011. The effect of multi-walled carbon nanotubes on soil microbial activity. Ecotoxicol. Environ. Saf. 74, 569–575.

Chung, H., Kim, M.J., Ko, K., Kim, J.H., Kwon, H., Hong, I., Park, N., Lee, S.W., Kim, W., 2015. Effects of graphene oxides on soil enzyme activity and microbial biomass. Sci. Total Environ. 514, 307–313.

Cui, X.Y., Jia, F., Chen, Y.X., Gan, J., 2011. Influence of single-walled carbon nanotubes on microbial availability of phenanthrene in sediment. Ecotoxicology 20, 1277–1285.

DeBruyn, J.M., Chewning, C.S., Sayler, G.S., 2007. Comparative quantitative prevalence of *Mycobacteria* and functionally abundant *nidA*, *nahAc*, and *nagAc* dioxygenase genes in coal tar contaminated sediments. Environ. Sci. Technol. 41, 5426–5432.

Ding, G.C., Heuer, H., Zuhlke, S., Spiteller, M., Pronk, G.J., Heister, K., Kogel-Knabner, I., Smalla, K., 2010. Soil type-dependent responses to phenanthrene as revealed by determining the diversity and abundance of polycyclic aromatic hydrocarbon ring-hydroxylating dioxygenase genes by using a novel PCR detection system. Appl. Environ. Microbiol. 76, 4765–4771.

Ferguson, P.L., Chandler, G.T., Templeton, R.C., DeMarco, A., Scrivens, W.A., Englehart, B.A., 2008. Influence of sediment-amendment with single-walled carbon nanotubes and diesel soot on bioaccumulation of hydrophobic organic contaminants by benthic invertebrates. Environ. Sci. Technol. 42, 3879–3885.

Ge, Y., Priester, J.H., Mortimer, M., Chang, C.H., Ji, Z.X., Schimel, J.P., Holden, P.A., 2016. Long-term effects of multi-walled carbon nanotubes and graphene on microbial communities in dry soil. Environ. Sci. Technol. 50, 3965–3974.

Ge, Y., Shen, C.C., Wang, Y., Sun, Y.Q., Schimel, J.P., Gardea-Torresdy, J.L., Holden, P.A., 2018. Carbonaceous nanomaterials have higher effects on soybean rhizosphere prokaryotic communities during the reproductive growth phase than during vegetative growth. Environ. Sci. Technol. 52, 6636–6646.

Harms, H., Schlosser, D., Wick, L.Y., 2011. Untapped potential: exploiting fungi in bioremediation of hazardous chemicals. Nat. Rev. Microbiol. 9, 177–192.

Holden, P.A., Klaessig, F., Turco, R.F., Priester, J.H., Rico, C.M., Avila-Arias, H., Mortimer, M., Pacpaco, K., Gardea-Torresdey, J.L., 2014. Evaluation of exposure concentrations used in assessing manufactured nanomaterial environmental hazards: are they relevant? Environ. Sci. Technol. 48, 10541–10551.

Jin, L.X., Son, Y., Yoon, T.K., Kang, Y.J., Kim, W., Chung, H., 2013. High concentrations of single-walled carbon nanotubes lower soil enzyme activity and microbial biomass. Ecotoxicol. Environ. Saf. 88, 9–15.

Jurelevicius, D., Alvarez, V.M., Peixoto, R., Rosado, A.S., Seldin, L., 2012. Bacterial polycyclic aromatic hydrocarbon ring-hydroxylating dioxygenases (PAH-RHD) encoding genes in different soils from King George Bay, Antarctic Peninsula. Appl. Soil Ecol. 55, 1–9.

Kobayashi, D.Y., Crouch, J.A., 2009. Bacterial/fungal interactions: from pathogens to mutualistic endosymbionts. Annu. Rev. Phytopathol. 47, 63–82.

Kostka, J.E., Prakash, O., Overholt, W.A., Green, S.J., Freyer, G., Canion, A., Delgardio, J., Norton, N., Hazen, T.C., Huettel, M., 2011. Hydrocarbon-degrading bacteria and the bacterial community response in Gulf of Mexico beach sands impacted by the Deepwater Horizon oil spill. Appl. Environ. Microbiol. 77, 7962–7974.

Liu, S.B., Wei, L., Hao, L., Fang, N., Chang, M.W., Xu, R., Yang, Y.H., Chen, Y., 2009. Sharper and faster "nano darts" kill more bacteria: a study of antibacterial activity of individually dispersed pristine single-walled carbon nanotube. ACS Nano 3, 3891–3902.

Moody, J.D., Freeman, J.P., Doerge, D.R., Ceriglia, C.E., 2001. Degradation of phenanthrene and anthracene by cell suspensions of *Mycobacterium* sp. strain PYR-1. Appl. Environ. Microbiol. 67, 1476–1483.

Niepceron, M., Portet-Koltalo, F., Merlin, C., Motelay-Massei, A., Barray, S., Bodilis, J., 2010. Both *cycloclasticus* spp. and *pseudomonas* spp. as PAH-degrading bacteria in the Seine estuary (France). FEMS Microbiol. Ecol. 71, 137–147.

Niepceron, M., Martin-Laurent, F., Crampon, M., Portet-Koltalo, F., Akpa-Vinceslas, M., Legras, M., Bru, D., Bureau, F., Bodilis, J., 2013. Gammaproteobacteria as a potential bioindicator of a multiple contamination by polycyclic aromatic hydrocarbons (PAHs) in agricultural soils. Environ. Pollut. 180, 199–205.

Nyberg, L., Turco, R.F., Nies, L., 2008. Assessing the impact of nanomaterials on anaerobic microbial communities. Environ. Sci. Technol. 42, 1938–1943.

Olajire, A.A., Essien, J.P., 2014. Aerobic degradation of petroleum components by microbial consortia. J. Pet. Environ. Biotechnol. 5, 195. https://doi.org/10.4172/2157-7463.1000195.

Oyelami, A.O., Semple, K.T., 2015. The impact of carbon nanomaterials on the development of phenanthrene catabolism in soil. Environ. Sci.: Processes Impacts 17, 1302–1310.

Petersen, E.J., Pinto, R.A., Landrum, P.F., Weber, J., Walter, J., 2009. Influence of carbon nanotubes on pyrene bioaccumulation from contaminated soils by earthworms. Environ. Sci. Technol. 43, 4181–4187.

Ren, G.D., Ren, W.J., Teng, Y., Li, Z.G., 2015. Evident bacterial community changes but only slight degradation when polluted with pyrene in a red soil. Front. Microbiol. 6, 22. https://doi.org/10.3389/fmicb.2015.00022.

Rodrigues, D.F., Elimelech, M., 2010. Toxic effects of single-walled carbon nanotubes in the development of *E. coli* biofilm. Environ. Sci. Technol. 44, 4583–4589.

Rodrigues, D.F., Jaisi, D.P., Elimelech, M., 2012. Toxicity of functionalized single-walled carbon nanotubes on soil microbial communities: implications for nutrient cycling in soil. Environ. Sci. Technol. 47, 625–633.

Salvo, V.S., Gallizia, I., Moreno, M., Fabiano, M., 2005. Fungal communities in PAH-impacted sediments of Genoa-Voltri Harbour (NW Mediterranean, Italy). Mar. Pollut. Bull. 50, 553–559.

Sawulski, P., Clipson, N., Doyle, E., 2014. Effects of polycyclic aromatic hydrocarbons on microbial community structure and PAH ring hydroxylating dioxygenase gene abundance in soil. Biodegradation 25, 835–847.

Shan, J., Ji, R., Yu, Y.J., Xie, Z.B., Yan, X.Y., 2015. Biochar, activated carbon, and carbon nanotubes have different effects on fate of ^{14}C-catechol and microbial community in soil. Sci. Rep. 5, 16000. https://doi.org/10.1038/srep16000.

Shen, M., Xia, X., Wang, F., Zhang, P., Zhao, X., 2012. Influences of multiwalled carbon nanotubes and plant residue chars on bioaccumulation of polycyclic aromatic hydrocarbons by *Chironomus plumosus* larvae in sediment. Environ. Toxicol. Chem. 31, 202–209.

Singh, H., 2006. Mycoremediation: Fungal Bioremediation. Wiley, Hoboken.

Tong, Z.H., Bischoff, M., Nies, L., Applegate, B., Turco, R.F., 2007. Impact of fullerene (C_{60}) on a soil microbial community. Environ. Sci. Technol. 41, 2985–2991.

Tong, Z.H., Bischoff, M., Nies, L.F., Myer, P., Applegate, B., Turco, R.F., 2012. Response of soil microorganisms to as-produced and functionalized single-walled carbon nanotubes (SWNTs). Environ. Sci. Technol. 46, 13471–13479.

Towell, M.G., Browne, L.A., Paton, G.I., Semple, K.T., 2011. Impact of carbon nanomaterials on the behaviour of ^{14}C-phenanthrene and ^{14}C-benzo-[a] pyrene in soil. Environ. Pollut. 159, 706–715.

Vance, E.D., Brookes, P.C., Jenkinson, D.S., 1987. Microbial biomass measurements in forest soils: the use of the chloroform fumigation-incubation method in strongly acid soils. Soil Biol. Biochem. 19, 697–702.

Vinas, M., Sabate, J., Espuny, M.J., Solanas, A.M., 2005. Bacterial community dynamics and polycyclic aromatic hydrocarbon degradation during bioremediation of heavily creosote-contaminated soil. Appl. Environ. Microbiol. 71, 7008–7018.

Walter, U., Beyer, M., Klein, J., Rehm, H.J., 1991. Degradation of pyrene by *Rhodococcus* sp. UW1. Appl. Microbiol. Biotechnol. 34, 671–676.

Wang, X.L., Liu, Y., Tao, S., Xing, B.S., 2010. Relative importance of multiple mechanisms in sorption of organic compounds by multiwalled carbon nanotubes. Carbon 48, 3721–3728.

Wang, X.L., Liu, Y., Zhang, H.Y., Shen, X.F., Cai, F., Zhang, M., Gao, Q., Chen, W.X., Wang, B., Tao, S., 2016. The impact of carbon nanotubes on bioaccumulation and translocation of phenanthrene, 3-CH_3-phenanthrene and 9-NO_2-phenanthrene in maize (*Zea mays*) seedlings. Environ. Sci.: Nano 3, 818–829.

Winquist, E., Björklöf, K., Schultz, E., Rasanen, M., Salonen, K., Anasonye, F., Cajthaml, T., Steffen, K.T., Jørgensen, K.S., Tuomela, M., 2014. Bioremediation of PAH-contaminated soil with fungi - from laboratory to field scale. Int. Biodeterior. Biodegrad. 86, 238–247.

Xia, X.H., Li, Y.R., Zhou, Z., Feng, C.L., 2010. Bioavailability of adsorbed phenanthrene by black carbon and multi-walled carbon nanotubes to *Agrobacterium*. Chemosphere 78,

1329–1336.
Xia, X.H., Zhou, C.H., Huang, J.H., Wang, R., Xia, N., 2013. Mineralization of phenanthrene sorbed on multi-walled carbon nanotubes. Environ. Toxicol. Chem. 32, 894–901.
Xia, X.H., Xia, N., Li, Y.J., Dong, J.W., Zhao, P.J., Zhu, B.T., Li, Z.H., Ye, W., Yuan, Y., Huang, J.X., 2015. Response of PAH-degrading genes to PAH bioavailability in the overlaying water, suspended sediment, and deposited sediment of the Yangze River. Chemosphere 128, 236–244.
Yang, K., Wang, X.L., Zhu, L.Z., Xing, B.S., 2006. Competitive sorption of pyrene, phenanthrene, and naphthalene on multiwalled carbon nanotubes. Environ. Sci. Technol. 40, 5804–5810.
Yang, Y., Shu, L., Wang, X.L., Xing, B.S., Tao, S., 2010. Effects of composition and domain arrangement of biopolymer compounds of soil organic matter on the bioavailability of phenanthrene. Environ. Sci. Technol. 44, 3339–3344.
Yang, F., Jiang, Q., Zhu, M.R., Zhao, L.L., Zhang, Y., 2017. Effects of biochars and MWNTs on biodegradation behavior of atrazine by *Acinetobacter lwoffii* DNS32. Sci. Total Environ. 577, 54–60.
Zeinali, M., Vossoughi, M., Ardestani, S.K., 2008. Naphthalene metabolism in *Nocardia otitidiscaviarum* strain TSH1, a moderately thermophilic microorganism. Chemosphere 72, 905–909.
Zhang, M., Shen, X.F., Zhang, H.Y., Cai, F., Chen, W.X., Gao, Q., Ortega-Calvo, J.J., Tao, S., Wang, X.L., 2016. Bioavailability of phenanthrene and nitrobenzene sorbed on carbonaceous materials. Carbon 110, 404–413.
Zhang, H.Y., Chen, W.X., Shen, X.F., Zhang, M., Yang, Y., White, J.C., Tao, S., Wang, X.L., 2017. Influence of multi-walled carbon nanotubes and fullerenes on the bioaccumulation and elimination kinetics of phenanthrene in geophagous earthworms (*Metaphire guillelmi*). Environ. Sci.: Nano 4, 1887–1899.
Zhou, W.Q., Shan, J., Jiang, B.Q., Wang, L.H., Feng, J.F., Guo, H.Y., Ji, R., 2013. Inhibitory effects of carbon nanotubes on the degradation of ^{14}C-2,4-dichlorophenol in soil. Chemosphere 90, 527–534.
Zhu, B.T., Wu, S., Xia, X.H., Lu, X.X., Zhang, X.T., Xia, N., Liu, T., 2016. Effects of carbonaceous materials on microbial bioavailability of 2,2′,4,4′-tetrabromodiphenyl ether (BDE-47) in sediments. J. Hazard. Mater. 312, 216–223.